The speed of vaccination rollout and the risk of pathogen adaptation

Sylvain Gandon[1,*], Amaury Lambert[2,3], Marina Voinson[1], Troy Day[4,5], and Todd L. Parsons[6]

[1]CEFE, CNRS, Univ Montpellier, EPHE, IRD, Montpellier, France

[*]Corresponding author

[2]Institut de Biologie de l'ENS (IBENS), École Normale Supérieure (ENS), CNRS UMR 8197, Paris, France

[3]Center for Interdisciplinary Research in Biology (CIRB), Collège de France, CNRS UMR 7241, INSERM U1050, PSL Research University, Paris, France

[4]Department of Mathematics and Statistics, Queen's University, Kingston, Canada

[5]Department of Biology, Queen's University, Kingston, Canada

[6]Laboratoire de Probabilités, Statistique et Modélisation (LPSM), Sorbonne Université, CNRS UMR 8001, Paris, France

Tuesday 12th March, 2024

E-mails: SG - sylvain.gandon@cefe.cnrs.fr; AL - amaury.lambert@ens.fr; MV - marina.voinson@hotmail.com; TD - tday@mast.queensu.ca; TLP - todd.parsons@upmc.fr;

Keywords: evolutionary epidemiology, vaccination, life-history evolution, demographic stochasticity, virulence, adaptive dynamics

Abstract

Vaccination is expected to reduce disease prevalence and to halt the spread of epidemics. But pathogen adaptation may erode the efficacy of vaccination and challenge our ability to control disease spread. Here we examine the influence of the speed of vaccination rollout on the overall risk of pathogen adaptation to vaccination. We extend the framework of evolutionary epidemiology theory to account for the different steps leading to adaptation to vaccines: (1) introduction of a vaccine-escape variant by mutation from an endemic wild-type pathogen, (2) invasion of this vaccine-escape variant in spite of the risk of early extinction, (3) spread and, eventually, fixation of the vaccine-escape variant in the pathogen population. We show that the risk of pathogen adaptation is maximal for intermediate speed of vaccination rollout. On the one hand, slower rollout decreases pathogen adaptation because selection is too weak to avoid early extinction of the new variant. On the other hand, faster rollout decreases pathogen adaptation because it reduces the influx of adaptive mutations. Hence, vaccinating faster is recommended to decrease both the number of cases and the likelihood of pathogen adaptation. We also show that pathogen adaptation is driven by its basic reproduction ratio, the efficacy of the vaccine and the effects of the vaccine-escape mutations on pathogen life-history traits. Accounting for the interplay between epidemiology, selection and genetic drift, our work clarifies the influence of vaccination policies on different steps of pathogen adaptation and allows us to anticipate the effects of public-health interventions on pathogen evolution.

Significance statement: Pathogen adaptation to host immunity challenges the efficacy of vaccination against infectious diseases. Are there vaccination strategies that limit the emergence and the spread of vaccine-escape variants? Our theoretical model clarifies the interplay between the timing of vaccine escape mutation events and the transient epidemiological dynamics following the start of a vaccination campaign on pathogen adaptation. We show that the risk of adaptation is maximized for intermediate vaccination coverage but can be reduced by a combination of non pharmaceutical interventions and faster vaccination rollout.

1 Introduction

Vaccination offers unique opportunities to protect a large fraction of the host population and thus to control spreading epidemics. In principle, large vaccination coverage can lead to pathogen eradication. In practice, however, the coverage required for eradication is often impossible to reach with imperfect vaccines [16, 34]. Moreover, pathogen adaptation may erode the efficacy of vaccination. Even if adaptation to vaccines is less common than adaptation to drugs [14, 26, 27] the spread of vaccine-escape mutations may challenge our ability to halt the spread of epidemics.

Understanding the dynamics of pathogen adaptation to vaccines is particularly relevant in the control of the ongoing SARS-CoV-2 pandemic. Yet, most theoretical studies that explore the evolution of pathogens after vaccination are based on the analysis of deterministic models and ignore the potential effects induced by the stochasticity of epidemiological dynamics. Demographic stochasticity, however, drives the intensity of genetic drift and can affect the establishment of new mutations and the long-term evolution of pathogens [42, 44, 41]. Several studies showed how the demographic stochasticity induced by finite host and pathogen population sizes alters selection on the life-history traits of pathogens [29, 22, 36]. These analytical predictions rely on the assumption that mutation rate is low, which allows us to decouple epidemiological and evolutionary time scales. Indeed, when the influx of new mutations is low, the new strain is always introduced after the resident pathogen population has reached its endemic equilibrium. Many pathogens, however, have relatively large mutation rates [43] and the fate of a pathogen mutant introduced away from the endemic equilibrium is likely to be affected by the dynamics of the pathogen populations. Besides, the start of a vaccination campaign is expected to yield massive perturbations of the epidemiological dynamics and new mutations are likely to appear when the pathogen population is far from its endemic equilibrium.

The aim of the present study is to develop a versatile theoretical framework to evaluate the consequences of vaccination on the risk of pathogen adaptation to vaccination. There are six main evolutionary epidemiology outcomes after the start of vaccination which are summarized in **Figure 1**. Some of these outcomes are more favorable than others because they do not lead to the invasion of a new variant (**Figure 1a-c**). In contrast, vaccination may lead to the invasion of

vaccine-escape variants (**Figure 1e-f**). In the following we use a combination of deterministic and branching process approximations to study the joint epidemiological and evolutionary dynamics of the pathogen population. This analysis reveals the importance of the speed of the vaccination rollout as well as of the life-history characteristics of the vaccine-escape variants on the probability of pathogen adaptation.

2 Model

We use a classical SIR epidemiological model with demography, where hosts can either be susceptible, infected or recovered [3]. The discrete number of each of these types of hosts is denoted by S^n, I^n and R^n, respectively. Because we are interested in the effect of demographic stochasticity the model is derived from a microscopic description of all the events that may occur in a finite—but not fixed—host population of (varying) total size $N^n = S^n + I^n + R^n$. We consider a continuous-time Markov process tracking the number of individuals of each type of host (see SI Section 1 for a detailed description). The susceptible hosts immigrate at rate λn, where n is a "system size", or scaling parameter, that indicates the order of magnitude of the arena in which the epidemic occurs. Hence the total host population varies stochastically in time, but remains of the order of n.

Vaccination may either take place with probability p when a new susceptible host enters the population (e.g., early childhood vaccination) or at a constant rate ν for all other susceptible hosts (e.g., vaccination of adults). The immunity triggered by vaccination is assumed to wane at rate ω_V, and natural immunity is assumed to wane at rate ω_R. A host may be unvaccinated, U, or vaccinated, V, and may either be uninfected or infected with the wild type, w, or a mutant strain, m (we assume coinfections are not possible). We thus have to track the numbers of two classes of susceptible hosts (S^n_U, S^n_V, where $S^n = S^n_U + S^n_V$) and four classes of infected individuals ($I^n_{Uw}, I^n_{Um}, I^n_{Vw}, I^n_{Vm}$, where $I^n = \sum_i I^n_{Ui} + I^n_{Vi}$). Recovered individuals are assumed to be fully protected (no reinfections) because natural immunity is expected to be more effective than immunity triggered by vaccination (we relax this assumption at the end of the paper). We further assume that the virulence α_i (the mortality rate induced by the infection), the transmission β_i (the production rate of new infections), and the recovery γ_i (the rate at which the host clears the infection) are fully

governed by the pathogen genotype ($i = w$ or m). A fourth trait $\epsilon_i \in [0, 1]$ governs the infectivity of pathogen genotype i on vaccinated hosts (infectivity of all genotypes is assumed to be equal to 1 on unvaccinated hosts). In other words, this final trait measures the ability of the pathogen to escape the immunity triggered by the vaccine. Note that these assumptions allow us to aggregate infected hosts irrespective of their vaccination status which simplifies the analysis below. For simplicity we assume frequency-dependent transmission where the number of contacts a host may have in the population is constant, but a proportion of those contacts may be infectious. Note, however, that other forms of transmission (e.g. density-dependent transmission [33]) are expected to yield qualitatively similar results. We summarize the states of the process and the jump rates at which individuals transition between states in **Table S1** and in **Figure 2**.

We use this model to examine the epidemiological and evolutionary dynamics following the start of a vaccination campaign. For the sake of simplicity, we focus our analysis on scenarios where the pathogen population has reached an endemic equilibrium before the start of vaccination. This is a strong assumption but our aim in this study is to focus on a simple scenario to understand the interplay between epidemiology and the stochastic fate of vaccine escape mutations. This is a necessary first step before studying more complex scenarios where vaccination starts before the epidemic has reached an endemic equilibrium. Note that we explore the robustness of our results at the end of the paper after relaxing some of our simplifying assumptions (see section 5.6).

Before going further in the analysis of the model we detail the default parameter values used to explore numerically the dynamics of viral adaptation in the figures presented in the following section (**Table 1**). We chose parameter values consistent with an acute viral infections of humans (e.g. SARS-CoV, Influenza...). The average lifespan of infected hosts is 64 years ($\lambda = \delta = 3\ 10^{-4}\ week^{-1}$) and the average duration of infection is 3.5 days ($\gamma_w = 2\ week^{-1}$). The case mortality of the wild type virus is assumed to be $\approx 1\%$ (i.e. $\alpha_w/(\alpha_w + \gamma_w)$ and has a basic reproduction ratio of $R_w = \beta_w/(\delta + \alpha_w + \gamma) \approx 5$. The immunity triggered by the infection or by the vaccination is around 4.5 months ($\omega_R = \omega_V = 0.05\ week^{-1}$) . The wild type virus is assumed to have a low probability to infect vaccinated hosts ($\epsilon_w = 0.05$). As explained in the following section, we varied the phenotypic properties of the mutant virus but, crucially, we focused on mutants with the ability

to escape the immunity triggered by vaccination ($\epsilon_m = 1$) and a lower basic reproduction ratio than the wild type in a fully susceptible population (i.e. adaption to vaccination is assumed to cary some fitness cost).

3 Results

3.1 Deterministic Approximation

As a first step in our analysis, we use a deterministic approximation for large values of n [30] and we work with host densities defined as $S_i = S_i^n/n$, $I_{ij} = I_{ij}^n/n$, $N = N^n/n$. This corresponds to replacing discrete individuals by densities and interpreting the rates in **Figure 2** as describing continuous flows rather than jumps. This yields a system of ordinary differential equations:

$$
\begin{aligned}
\dot{S}_U &= \lambda(1-p) + \omega_V S_V + \omega_R R - \left(\beta_w \frac{I_{Uw} + I_{Vw}}{N} + \beta_m \frac{I_{Um} + I_{Vm}}{N} + \delta + \nu\right) S_U \\
\dot{S}_V &= \lambda p + \nu S_U - \left(\epsilon_w \beta_w \frac{I_{Uw} + I_{Vw}}{N} + \epsilon_m \beta_m \frac{I_{Um} + I_{Vm}}{N} + \delta + \omega_V\right) S_V \\
\dot{I}_{Uw} &= \beta_w (I_{Uw} + I_{Vw}) \frac{S_U}{N} - (\delta + \alpha_w + \gamma_w) I_{Uw} \\
\dot{I}_{Um} &= \beta_m (I_{Um} + I_{Vm}) \frac{S_U}{N} - (\delta + \alpha_m + \gamma_m) I_{Um} \\
\dot{I}_{Vw} &= \epsilon_w \beta_w (I_{Uw} + I_{Vw}) \frac{S_V}{N} - (\delta + \alpha_w + \gamma_w) I_{Vw} \\
\dot{I}_{Vm} &= \epsilon_m \beta_m (I_{Um} + I_{Vm}) \frac{S_V}{N} - (\delta + \alpha_m + \gamma_m) I_{Vm} \\
\dot{R} &= (\gamma_w I_{Uw} + \gamma_w I_{Vw} + \gamma_m I_{Um} + \gamma_m I_{Vm}) - (\delta + \omega_R) R,
\end{aligned}
\tag{1}
$$

It is also convenient to track the dynamics of the total density of hosts infected with the same strain i, $I_i := I_{Ui} + I_{Vi}$, which yields:

$$
\dot{I}_i = \underbrace{\left(\left(\beta_i \frac{S_U}{N} + \epsilon_i \beta_i \frac{S_V}{N}\right) - (\delta + \alpha_i + \gamma_i)\right)}_{r_i = \text{growth rate of strain } i} I_i \tag{2}
$$

The ability of the strain i to grow is given by the sign of the growth rate r_i. Note that this growth rate depends on the four different traits of the pathogen: $\alpha_i, \beta_i, \gamma_i, \epsilon_i$. But this growth rate depends

also on the densities S_U and S_V, which vary with t, the time since the start of vaccination (i.e., vaccination starts at $t = 0$). The coefficient of selection s_m on the mutant strain relative to the wild type is:

$$s_m = r_m - r_w = (\beta_m - \beta_w)\frac{S_U}{N} + (\epsilon_m\beta_m - \epsilon_w\beta_w)\frac{S_V}{N} - (\alpha_m - \alpha_w + \gamma_m - \gamma_w) \tag{3}$$

In other words, both the genetics (the phenotypic traits of strain i) and the environment (the epidemiological state of the host population) govern selection and strain dynamics.

3.2 Pathogen eradication and vaccination threshold

The ability of the strain i to grow can be measured by its effective per-generation reproduction ratio which is given by:

$$R_i^e = R_i\left(\frac{S_U}{N} + \epsilon_i\frac{S_V}{N}\right) \tag{4}$$

where $R_i = \frac{\beta_i}{\delta+\alpha_i+\gamma_i}$. Hence, a reduction of the availability of susceptible hosts with vaccination may drive down the density of the wild-type pathogen when the production of new infected hosts (infection "birth") does not compensate for the recovery and death of infected hosts (infection "death"), that is when $R_w^e < 1$. Ultimately, vaccination can even lead to the eradication of the wild-type pathogen (**Figure 1a**) either when the vaccine is sufficiently efficient ($\epsilon_w R_w > 1$) or when the vaccination coverage is sufficiently high [34, 16]. The deterministic model (1) can be used to identify the threshold ν_c of the speed of vaccination rollout above which the wild-type pathogen can be driven to extinction (see Methods and SI Section 1):

$$\nu_c = \frac{R_w(\delta(1-(1-\epsilon_w)p) + \omega_V) - (\delta + \omega_V)}{1 - R_w\epsilon_w} \tag{5}$$

As expected, better vaccines (i.e., lower values of ϵ_w and ω_V) yield lower threshold values for the speed of vaccination. Imperfect vaccines (i.e., higher values of ϵ_w and ω_V), in contrast, are unlikely to allow eradication. Note that, if we wait sufficiently long, the population of the wild-

type pathogen will be driven to extinction in a *stochastic* way even when $\nu < \nu_c$. Indeed, in a finite host population, sooner or later, the pathogen population is doomed to go extinct because of demographic stochasticity, but the extinction time when $\nu < \nu_c$ will usually be very long, increasing exponentially with the system size n. From now on, we are going to neglect the possibility of extinction of the wild type due to vaccination when $\nu < \nu_c$ (which is a good approximation when n is large).

The spread of a new pathogen variant may erode the efficacy of vaccination and, consequently, could affect the ability to control and, ultimately, to eradicate the pathogen. But before the replacement of the wild type by a vaccine-escape variant the pathogen population may go through three steps that may ultimately result (or not) in pathogen adaptation: (1) introduction of the vaccine-escape variant by mutation, (2) extinction (**Figure 1c**) or invasion (**Figure 1d-f**) of the vaccine-escape variant introduced by mutation, (3) fixation (**Figure 1f**) or not (**Figure 1d-e**) of the invading vaccine-escape variant. Each of these steps is very sensitive to stochasticity because the number of vaccine-escape variants is very small in the early phase of its emergence.

3.3 Step 1: Introduction of the variant by mutation

The first step of adaptation is driven by the production of new variants by the wild-type pathogen through mutation. The level of adaptation to unvaccinated and vaccinated hosts may vary among those variants [10]. Vaccine-escape mutations that do not carry any fitness costs (or may even be adaptive) in unvaccinated hosts are expected to invade and fix relatively easily irrespective of the vaccination strategy. We thus focus on variants that carry fitness costs in immunologically naïve hosts (i.e., variants *specialized* on vaccinated hosts [10]). In principle, the introduction of the vaccine-escape mutation may occur before the rollout of vaccination. The distribution of these mutations is expected to follow a stationary distribution resulting from the action of recurrent mutations and negative selection (see Methods). If these fitness costs are high and/or if the mutation rate is low these pre-existing mutants are expected to be rare. In the following, we neglect the presence of pre-existing mutants and we focus on a scenario where the first vaccine-escape mutant appears after the start of vaccination (but see Methods, section 5.5 where we discuss the effect of

standing genetic variation).

At the onset of the vaccination campaign (i.e., $t = 0$) we assume that the system is at the endemic equilibrium (i.e., the equilibrium densities S_U^0, I_{Uw}^0 and I_{Vw}^0 are given in (13) in the Methods). We assume that an individual host infected with the wild type produces vaccine-escape mutants at a small, constant rate θ_U/n if unvaccinated and θ_V/n if vaccinated. We assume that θ_U and θ_V are small enough that within-host clonal interference among vaccinated-adapted variants is negligible. The relative rates of mutation in the two types of hosts is unknown but the within-host selection may favor mutants in vaccinated hosts which may yield $\theta_V \geq \theta_U$. However, the lower viral load in vaccinated host may counteract this effect and may yield $\theta_U \geq \theta_V$. The total production of mutants is thus equal to $\frac{\theta_U}{n} I_{Uw}^n(t) + \frac{\theta_V}{n} I_{Vw}^n(t) \approx \theta_U I_{Uw}(t) + \theta_V I_{Vw}(t)$, so that the probability density $f_m(t)$ of the arrival time $t = t_m$ of the first vaccine-escape mutant is approximated by:

$$f_m(t) = \left(\theta_U I_{Uw}(t) + \theta_V I_{Vw}(t)\right) e^{-\int_0^t (\theta_U I_{Uw}(s) + \theta_V I_{Vw}(s))\, ds}. \tag{6}$$

In other words, the time t_m at which the vaccine-escape variant is first introduced by mutation depends on the dynamics of the incidence of the infections by the wild type. Plots of f_m for different values of rollout speed ν in **Figure 3** show that a faster rollout of vaccination delays the introduction of the vaccine-escape mutant. This effect is particularly marked when $\omega_R = 0$ because life-long immunity is known to result in a massive transient drop of the incidence (the honey-moon period) [34, 13] which is expected to decrease the influx of new variants during this period (**Figure S1**). **Figure 3** also shows how higher values of θ_V can increase the influx of vaccine-escape variants. As discussed in the following section, the subsequent fate of vaccine-escape mutants depends strongly on the timing of their arrival.

3.4 Step 2: Variant invasion

Immediately after its introduction, the dynamics of the vaccine-escape mutant may be approximated by a time-inhomogeneous birth-death process where the rate of birth (i.e., rate of new infections by the mutant) varies with the availability of susceptible hosts (see Methods, section 5.3). The probability that a single mutant with time-varying birth rate $b_m(t) = \beta_m \left(\frac{S_U(t)}{N(t)} + \frac{\epsilon_m S_V(t)}{N(t)}\right)$ and

constant death rate $d_m = \delta + \alpha_m + \gamma_m$, introduced at time t_m, successfully invades (see [25] and SI, Section 2) is:

$$P_m^{t_m} = \frac{1}{1 + \int_{t_m}^{\infty} d_m e^{-\int_{t_m}^{t} b_m(s) - d_m \, ds} \, dt} \tag{7}$$

Plotting the probability of invasion against t_m in **Figure 4** shows that the time at which the vaccine-escape mutant is introduced has a dramatic impact on the probability of escaping early extinction. If the mutant is introduced early, the density $S_V(t)$ of susceptible vaccinated hosts remains very low and the selection for the vaccine-escape mutant is too small to prevent stochastic extinctions. The probability of invasion increases with selection, and thus with the density of vaccinated hosts, which tends to increase with time (see equation (3)).

Taking $t_m \to \infty$ allows us to tackle the situation when the vaccine-escape mutant appears at the endemic equilibrium, i.e., when the densities of unvaccinated and vaccinated susceptible hosts are $S_U^\star$ and $S_V^\star$, respectively. At that point in time the effective per-generation reproduction ratio of genotype i (i.e. the expected number of secondary infections produced by pathogen genotype i) is:

$$R_i^\star = R_i \left(\frac{S_U^\star}{N^\star} + \epsilon_i \frac{S_V^\star}{N^\star} \right) \tag{8}$$

By definition, at the endemic equilibrium set by the wild-type pathogen we have $R_w^\star = R_w^e = 1$. Hence, a necessary condition for the mutant to invade this equilibrium is $R_m^\star > 1$, i.e., the effective reproduction number of the mutant has to be higher than that of the wild type (see SI, Section 1). However, this is not a sufficient condition: many mutants that satisfy this condition will rapidly go extinct due to demographic stochasticity. But in contrast to an early introduction of the mutant discussed above, the stochastic dynamics of the mutant is approximately a *time-homogeneous* branching process because the birth rate of the mutant approaches $b_m^\star = \beta_i \left(\frac{S_U^\star}{N^\star} + \epsilon_i \frac{S_V^\star}{N^\star} \right)$. This birth rate is constant because the density of susceptible hosts remains constant at the endemic equilibrium. The probability of mutant invasion after introducing a single host infected by the mutant is thus (see SI Section 1; **Figure 4**):

$$P_m^\star = \lim_{t_m \to \infty} P_m^{t_m} = 1 - \frac{R_w^\star}{R_m^\star} = 1 - \frac{1}{R_m^\star} \tag{9}$$

Note that we recover the strong-selection result of [36]. This expression shows that *at this endemic equilibrium* the fate of the mutant is fully governed by the per-generation reproduction ratio of the two strains, but does not depend on the specific values of the life-history traits of the mutant (provided the different vaccine-escape variants have the same value of $R_m^\star$).

Interestingly, unlike $P_m^\star$, the probability $P_m^{t_m}$ of mutant invasion at time t_m given in (7) is not governed solely by R_i, but rather depends on the life-history traits of the mutants. For instance, assume that two vaccine-escape mutants have the same values of R_m and ϵ_m but they have very different life-history strategies. The "slow" strain has low rates of transmission and virulence (in green in **Figure 4**) while the "fast" strain has high rates of transmission and virulence (in red in **Figure 4**). **Figure 4** shows that the high mortality rate of hosts infected by the fast strain increases the risk of early extinction and lowers the probability of invasion relative to the slow strain. Hence, in the early stage of adaptation, pathogen life-history matters and favours slow strains with lower rates of transmission and virulence.

3.5 Step 3: After variant invasion

Successful invasion of the vaccine-escape mutant means that it escaped the "danger zone" when its density is so low that it is very likely to go extinct (**Figure 1d-f**). After this invasion we can describe the dynamics of the polymorphic pathogen population using the deterministic approximation (1).

Because the invasion of the mutant at the endemic equilibrium set by the wild type requires that $R_m^\star > R_w^\star$, we may expect from the analysis of the deterministic model that the mutant would always replace the wild-type pathogen. That is, the wild-type pathogen would go extinct before the mutant (**Figure 1f**). This is indeed the case when the phenotypes of the mutant and the wild type are not very different because of the "invasion implies fixation" principle [17, 5, 38]. Yet, this principle may be violated if the phenotype of the vaccine-escape mutant is very different than the phenotype of the wild type.

First, the long-term coexistence of the two genotypes is possible (**Figure 1e**).The coexistence requires that each genotype is specialized on distinct types of host. The wild-type is specialised on unvaccinated hosts (i.e. $R_w > R_m$) and the mutant is specialised on the vaccinated hosts (i.e.

$\epsilon_m > \epsilon_w$). Intermediate rates of vaccination maintain a mix of vaccinated and unvaccinated host wich promotes coexistence between the two genotypes (**Figure S2**). Second, the vaccine-escape mutant may be driven to extinction before the wild type if its life-history traits induce massive epidemiological perturbations after its successful invasion (**Figure 1d**). As pointed out by previous studies, more transmissible and aggressive pathogen strategies may yield larger epidemics because the speed of the epidemic is governed by the per-capita growth rate r_i, not by the per-generation reproduction ratio R_i [13]. This explosive dynamics is driven by an over-exploitation of the host population and is immediately followed by a massive decline in the incidence of the vaccine-escape mutant. In a finite host population, this may result in the extinction of the vaccine-escape mutant before the wild type [42]. We capture this outcome with a hybrid analytical-numerical approach that computes the probability $P_{fix}^{t_m}$ that the wild type will go extinct before the mutant (see Methods, section 5.4). **Figure 5** shows that two vaccine-escape mutants may have very different probabilities of fixation, even if they have the same per-generation reproduction ratio. The numerical computation of the probability of fixation agrees very well with individual-based stochastic simulations. The faster strain is unlikely to go to fixation because invasion is followed by a period where the birth rate drops to very low levels (far below the mortality rates, **Figure S3**). In other words, a more aggressive strategy will more rapidly degrade its environment, by depleting susceptible hosts, which is known to increase the probability of extinction [6]. Interestingly, this effect is only apparent when the time of introduction t_m is large. Indeed, when the mutant is introduced soon after the start of vaccination, its probability of invasion is already very low because its initial growth rate is negative (**Figure S3a, b, c**). When the mutant is introduced at intermediate times, the initial growth rate of the mutant is positive because some hosts are vaccinated (**Figure S3d, e, f**). If the vaccine-escape mutant is introduced later, the growth rate of the mutant is initially very high as many hosts are vaccinated (and thus susceptible to the vaccine-escape mutant) but this is rapidly followed by a drop in host density (especially pronounced with the faster strain) which prevents the long-term establishment of the faster strain (see **Figure S3g, h, i**).

3.6 The overall risk of pathogen adaptation

The overall probability that the pathogen will adapt to vaccination (*i.e.* that a vaccine-escape variant invades and eventually replace or coexist with the wild-type) depends upon the probability that the mutation will arise (step 1) and the probability that this mutation will escape early extinction (step 2) and eventually go to fixation (step 3). It is particularly relevant to explore the effect of the speed of vaccination rollout on the overall probability that some vaccine-escape variant invades before a time t after the start of the vaccination campaign (steps 1 and 2, **Figure 6**):

$$A_m^t = 1 - e^{-\int_0^t (\theta_U I_{Uw}(s) + \theta_V I_{Vw}(s)) P_m^s \, ds}. \tag{10}$$

When $\nu > \nu_c$, vaccination is expected to eradicate the disease rapidly. But an escape mutation may appear by mutation before eradication and rescue the pathogen population. This scenario fits squarely within the framework of classical "evolutionary rescue" modeling [32, 2, 4]. Yet, vaccination rollout is unlikely to be fast enough to eradicate the wild-type pathogen and, in this case, the probability of adaptation goes to 1 when $t \to \infty$. Indeed, when $\nu < \nu_c$, a vaccine-escape variant will eventually appear by mutation and invade. But what is less clear is how fast this adaptation will take place. We can use equation (10) to explore the effect of the speed of adaptation on the probability of pathogen adaptation at time t after the start of vaccination (i.e. the speed of adaptation). Crucially, the speed of pathogen adaptation is maximized for intermediate values of the speed of vaccination rollout. This is due to the antagonistic consequences the speed of the rollout has upon these two steps of adaptation (compare **Figures 3 and 4**). Faster rollout reduces the influx of new mutations, but increases selection for vaccine-escape mutations.

To illustrate this ambivalent effect we can first examine how the speed of vaccination rollout decreases the probability M_m^t that at least one escape mutation is introduced before time t (blue curve in **Figure 6**):

$$M_m^t = 1 - e^{-\int_0^t (\theta_U I_{Uw}(s) + \theta_V I_{Vw}(s)) \, ds}. \tag{11}$$

Second, we can examine how the speed of vaccination rollout increases the probability that a mutant invades which can be approximated by $P_m^\star$ (see equation (9)) when t is sufficiently large (purple

curve in **Figure 6**). The overall probability of adaptation can be well approximated by:

$$A_m^t \approx 1 - e^{-\int_0^t (\theta_U I_{Uw}(s) + \theta_V I_{Vw}(s))\, ds\, P_m^\star} \approx M_m^t P_m^\star. \tag{12}$$

This approximation captures how the speed of adaptation results from the balance between the influx of new mutations and the invasion success of these mutations. Interestingly, for low speed of vaccination rollout, the invasion of the escape mutant may not necessarily lead to the fixation of the new variant. Indeed, with low vaccination rollout yields a large fraction of the host population remains naïve and this heterogeneity can promote the coexistence between two specialist pathogens: the wild-type is specialised on naive hosts and the escape mutant is specialised on vaccinated hosts (**Figure S2**).

4 Discussion

Vaccination is a powerful tool to control the spread of infectious diseases, but some pathogens evolve to escape the immunity triggered by vaccines (e.g. flu, SARS-CoV-2). Will they continue to adapt to the different vaccines that are being used to halt their spread? Does the likelihood of this adaptation depend on the speed of the vaccination rollout? To answer these questions we must first understand the different steps that may eventually lead to adaptation to vaccination.

Mutation is the fuel of evolution, and the first step of adaptation to vaccination is the mutational process that produces vaccine-escape variants. Even if initial estimates of SARS-CoV-2 mutation rates were reassuringly low [39], the virus has managed to evolve higher rates of transmission [9, 46] and these adaptations are challenging current control measures used to slow down the ongoing pandemic. The ability of the new variants of SARS-CoV-2 to escape immunity is also worrying and indicates that viral adaption can weaken vaccine efficacy [47, 37]. The rate at which these potential vaccine-escape mutations are introduced depends on the density of hosts infected by the wild-type virus. In this respect, a faster rollout of vaccination is expected to delay the arrival of these mutations (**Figure 3**).

Some authors have argued that the emergence of vaccine-escape mutations may be more likely

in infected hosts which are partially immunized [12, 8, 10]. Our model can be used to explore the consequences of this within-host evolution in vaccinated hosts (*e.g.*, taking $\theta_V > \theta_U$). A larger value of θ_V increases the overall rate of mutation (**Figure 3**) but this effect is modulated by the fraction of the host population that is vaccinated. Consequently, when $\theta_V > \theta_U$, the speed of vaccination rollout can have a non-monotonic effect on the probability that a vaccine-escape mutation is introduced (see **Figure S4**). Indeed, when the rate of vaccination remains low, the enhancing effect of vaccination on the rate of introduction of new mutations can counteract the delaying effect of faster vaccination rollout discussed above. But the probability that a vaccine-escape mutation is introduced drops to very low levels when the rate of vaccination becomes overwhelmingly high.

The second step of adaptation starts as soon as the vaccine-escape mutant has been introduced in the pathogen population. Will this new variant go extinct rapidly or will it start to invade? The answer to this question depends on the time at which the mutant is introduced. If the mutant is introduced when the population is not at an endemic equilibrium, the fate of the mutant depends on a time-varying birth rate which is driven by the fluctuations of the density of susceptible hosts. In our model early introductions are likely to result in rapid extinction because there are simply not enough vaccinated hosts to favour the mutant over the wild type. Moreover, we found that earlier introductions are likely to favour slower life-history strategies which are less prone to early extinction. If the introduction takes place later, when the system has reached a new endemic equilibrium, the fate of the mutant is solely governed by the effective per-generation ratio $R_m^\star$ and does not depend on the life-history traits of the mutant. Slow and fast variants have equal probability to invade if they have the same $R_m^\star$. Altogether, our results suggest that earlier arrival may not always facilitate invasion since the probability of invasion is limited by the time-varying epidemiological state of the host population.

The third step of adaptation starts as soon as the hosts infected by the vaccine-escape mutant are abundant and the effect of demographic stochasticity on the dynamics of this mutation becomes negligible. Our analysis attempts to better characterize the dynamics of the mutant after invasion using a combination of deterministic and analytical approximations. In principle, conditional on invasion, we can use the deterministic model (1) to describe the joint dynamics of the mutant and

the wild type. In particular, the speed at which the vaccine-escape mutant spreads in the pathogen population can be well approximated by the deterministic model. This may be particularly useful to address the impact of various vaccination strategies on the speed of the spread of a vaccine-escape variant [15]. In the present work we show that life-history traits of the vaccine-escape mutant drive the speed of its spread. Indeed, as pointed out before, the deterministic transient dynamics depends on the per-capita growth rate of the mutant r_m, not its per-generation reproduction ratio R_m [13]. Transient dynamics may favour a fast and aggressive variant because this life-history strategy may be more competitive away from the endemic equilibrium. Yet, this explosive strategy may be risky for the pathogen if it leads to epidemiological fluctuations that result in a massive drop in the number of infections. The consequences of such fluctuations on the extinction risk of the variant can be accounted for by a generalized birth-death process where the per-capita growth rate of the mutant varies with time. Epidemiological fluctuations lead to a degradation of the future environment (i.e., depletion of the density of susceptible hosts) which results in an increased risk of extinction [25, 6].

A comprehensive understanding of pathogen dynamics after vaccination relies on the use of a combination of theoretical tools to capture the interplay between stochastic and deterministic forces. Here, we use a hybrid numerical-analytical approach to account for the three successive steps that may eventually lead to the fixation of a vaccine-escape mutant. This theoretical framework is particularly suitable to explore the influence of different vaccination strategies on the risk of pathogen adaptation. In particular, we show that this risk drops to very low levels even when the speed of vaccination rollout is below the threshold value that may eventually lead to eradication (i.e., $\nu < \nu_c$). In other words, faster vaccination rollout makes sense even when eradication is infeasible, because faster rollout decreases both the number of cases and the likelihood of pathogen evolution. This conclusion is akin to the general prediction that the rate of pathogen adaptation should be maximized for intermediate immune pressure or for medium doses of chemotherapy at the within-host level [20, 40, 19, 1, 21, 11, 2]. Most of these earlier studies focused on evolutionary rescue scenarios where the wild type is expected to be rapidly driven to extinction by human intervention. Our versatile theoretical framework, however, allows us to deal with a broader range of situations

where the intervention is not expected to eradicate the wild type pathogen. Accounting for the dynamics of the wild type affects both the flux of mutation and the fate of these mutations.

The framework we have developed can be readily extended to explore may other situations. For instance, our model can be modified to explore the influence of temporal variations in the environment that could be driven by seasonality or by non-pharmaceutical interventions (NPIs). We explored a situation where the transmission rate of all variants is periodically reduced by a quantity $1-c(t)$, where $c(t)$ is a measure of the intensity of NPIs. These periodic interventions affect both the flux of mutations and the probability that these mutations invade. In particular, NPIs lower the probability of mutant introduction through the reduction in the density of hosts infected by the wild type (**Figure S4**). As a consequence, the probability of adaptation is reduced when vaccination is combined with periodic control measures. Hence, our approach helps to understand the interaction between vaccination and NPI discussed in earlier studies [41, 31].

We have made several simplifying assumptions that need to be relaxed to confidently apply our findings to a broader range of pathogens such as the current SARS-CoV-2 pandemic (see section 5.6 in the Methods). First, one should study situations where the pathogen population has not reached an endemic equilibrium when vaccination starts to be applied. We carried out additional simulations showing that starting the vaccination rollout sooner (i.e. just after the start of the epidemic) tends to promote the probability of invasion of the escape mutant (**Figure S5**). Indeed, at the onset of the epidemic the density of susceptible hosts is higher (i.e. the birth rate of the infection is high relative to the endemic equilibrium) and the risk of early extinction of the mutant is reduced. Second, it is important to relax the assumption that natural immunity is perfect. We carried out additional simulations showing that when naturally immune hosts, like vaccinated hosts, can be reinfected the probability of invasion of the escape mutant increases (**Figure S6**). This effect is particularly strong just after the start of vaccination. Indeed, if naturally immune hosts are equivalent to vaccinated hosts, selection to escape immunity is present even before the start of vaccination and one may thus expect the speed of adaptation to be much faster and to be relatively independent of the vaccination strategy. Another important extension of our model would be to study the effect of a diversity of vaccines in the host population. We did not explore this

effect in the present study but this diversity of immune profiles among vaccinated hosts could slow down pathogen adaptation if the escape of different vaccines requires distinct mutations [45, 7, 35]. Finally, it is important to recall that we focus here on a simplified scenario where we analyse the evolutionary epidemiology of an isolated population. In real-life situations the arrival time may depend more on the immigration of new variants from abroad than on local vaccination policies. The influence of migration remains to be investigated in spatially structured models where vaccination may vary among populations [18].

5 Methods

In this section, we present how extinction, invasion and fixation probabilities may be obtained under strong-selection assumptions when a mutant strain appears in a host-pathogen system that is away from its endemic equilibrium. Our essential tools are the deterministic ordinary differential equations (1) and birth-and-death approximations, which we discuss below. The former allows us to consider the situation when all strains are abundant, the latter when at least one strain is rare. We will limit ourselves to an informal treatment, presenting heuristic arguments and deferring rigorous proofs and sharp error bounds to a future treatment. In the following we present a simple, yet versatile, hybrid (i.e., semi-deterministic) framework which allows us to approximate the probabilities associated with different steps of adaptation (mutation, invasion, fixation) via adding auxiliary equations describing stochastic phenomena, to the deterministic ordinary differential equations describing the global population dynamics.

5.1 Before the introduction of a variant

We assume that vaccination starts after the monomorphic population of the wild-type pathogen has reached its endemic equilibrium,

$$
\begin{aligned}
S_U^0 &= \frac{\lambda(\delta+\gamma_w+\omega_R)}{\delta(\beta_w-\alpha_w)+\omega_R(R_w(\alpha_w+\delta)-\alpha_w)} \\
S_V^0 &= 0 \\
I_{Uw}^0 &= \frac{\lambda(R_w-1)(\delta+\omega_R)}{\delta(\beta_w-\alpha_w)+\omega_R(R_w(\alpha_w+\delta)-\alpha_w)} \\
I_{Vw}^0 &= 0 \\
R^0 &= \frac{\lambda(R_w-1)\gamma_w}{\delta(\beta_w-\alpha_w)+\omega_R(R_w(\alpha_w+\delta)-\alpha_w)}
\end{aligned}
\tag{13}
$$

We then use the following ordinary differential equations to track the deterministic dynamics of the wild-type pathogen using the endemic equilibrium before vaccination (13) as the initial condition:

$$
\begin{aligned}
\dot{S}_U &= \lambda(1-p)+\omega_V S_V+\omega_R R-\left(\beta_w\frac{I_{Uw}+I_{Vw}}{N}+\delta+\nu\right)S_U \\
\dot{S}_V &= \lambda p+\nu S_U-\left(\epsilon_w\beta_w\frac{I_{Uw}+I_{Vw}}{N}+\delta+\omega_V\right)S_V \\
\dot{I}_{Uw} &= \beta_w(I_{Uw}+I_{Vw})\frac{S_U}{N}-(\delta+\alpha_w+\gamma_w)I_{Uw} \\
\dot{I}_{Vw} &= \epsilon_w\beta_w(I_{Uw}+I_{Vw})\frac{S_V}{N}-(\delta+\alpha_w+\gamma_w)I_{Vw} \\
\dot{R} &= (\gamma_w I_{Uw}+\gamma_w I_{Vw})-(\delta+\omega_R)\,R \\
\dot{N} &= \lambda-\delta N-\alpha_w(I_{Uw}+I_{Vw}).
\end{aligned}
\tag{14}
$$

Letting $I_w = I_{Uw} + I_{Vw}$, we get from (14):

$$
\dot{I}_w = \beta_w(S_U+\epsilon_w S_V)\frac{I_w}{N}-(\delta+\alpha_w+\gamma_w)I_w.
$$

A new endemic equilibrium will thus be approached after vaccination if and only if the growth rate $r_w = \beta_w(S_U+\epsilon_w S_V)/N-(\delta+\alpha_w+\gamma_w)$ is positive, or equivalently if the effective per-generation reproduction ratio

$$
R_w^e = R_w\left(\frac{S_U}{N}+\epsilon_w\frac{S_V}{N}\right)
$$

is larger than 1, when S_U and S_V are taking their stationary values $\tilde{S}_U$ and $\tilde{S}_V$ in the absence of infection. Computing these values (see SI, Section 1) shows that $R_w^e > 1$ if and only if $e_w R_w > 1$

or $\nu > \nu_c$, where

$$\nu_c = \frac{R_w(\delta(1-(1-\epsilon_w)p)+\omega_V)-(\delta+\omega_V)}{1-R_w\epsilon_w} \tag{15}$$

Thus we see that if $\epsilon_w R_w < 1$ and the speed of the vaccination rollout is higher than the critical value ν_c the wild type will be driven to extinction.

For values of the vaccination rollout ν smaller than this threshold ν_c, or when $e_w R_w > 1$, the wild-type may also go extinct due to demographic stochasticity. We can neglect this possibility because the timescale of stochastic extinction from abundances of the order of n is much larger than those of the processes under consideration.

5.2 Introduction of the variant by mutation (step 1)

As indicated above, we use a time-inhomogeneous Poisson point process to model the influx of new mutations. The per capita rate of mutation is assumed to be constant through time but whether or not a mutant will escape extinction within a host may depend on the type of host. Indeed, a vaccine-escape mutation may have a higher probability to escape within-host extinction in vaccinated hosts. We account for this effect by making a distinction between θ_U and θ_V. If vaccine-escape mutations are more likely to escape extinction in vaccinated hosts we expect $\theta_V > \theta_U$. In other words, $\theta_V/\theta_U - 1$ is a measure of the within-host fitness advantage of the vaccine-escape mutant in vaccinated hosts (they are assumed to have the same within-host fitness in naïve hosts).

We can compute the probability that some of the vaccine-escape mutations are present as standing variation before the start of vaccination. When the resident population has reached its endemic equilibrium $(S_U^0, 0, I_{Uw}^0, 0, N^0)$, the number of mutants is approximated by a birth-and-death process with immigration, with birth rate $b_m^0 = \beta_m \frac{S_U^0}{N^0}$ and death rate $d_m = \delta + \alpha_m + \gamma_m$, and the "immigration" is actually mutations arising in the resident population, which occur at rate $\mu_m = \theta_U I_{Uw}^0$. Because we assume that in a fully naïve host population vaccine-escape mutations carry a fitness cost relative to the resident strain, we have $b_m^0 < d_m$. The number of mutants thus approximately follows a subcritical birth-and-death process with immigration, which is known to converge in distribution as $t \to \infty$ to a negative binomial stationary distribution [24]. The

probability that there are k infected individuals hosting the mutant pathogen at time $t = 0$ is thus:

$$p_k = \binom{k+r-1}{k}(1-R_m^0)^r(R_m^0)^k \tag{16}$$

where $r = \mu_m/b_m^0$ and $R_m^0 = b_m^0/d_m$. Hence the the expected number of vaccine-escape mutants already present at the start of vaccination is

$$\frac{\mu_m}{d_m - b_m}. \tag{17}$$

This result is analogous to the classical result that the expected frequency of deleterious mutations is of the form μ/s where μ is the rate of mutation towards deleterious mutants and s is the fitness cost of those deleterious mutants.

We can also compute the probability that no mutant is present at the start of vaccination:

$$p_0 = (1-R_m^0)^r \tag{18}$$

When either R_m^0 or r is small, $p_0 \approx 1$, and we can neglect the presence of preexisting mutants. Otherwise, we need to account for the possibility that one or more mutants are present at time $t = 0$, which we discuss in Section 5.5 below.

We now assume that there is no mutant present at the start of vaccination. We are interested in the law of the first time t_m at which a mutant appears. Because $\theta_U I_{Uw}(t) + \theta_V I_{Vw}(t)$ is the flux of vaccine-escape mutants from the wild-type population, by the exponential formula for Poisson point processes, we have [28]:

$$\mathbb{P}\{t_m > t\} = e^{-\int_0^t (\theta_U I_{Uw}(s) + \theta_V I_{Vw}(s))ds}. \tag{19}$$

We can numerically compute the probability density function f_m of the firstarrival time t_m of a vaccine-escape mutant using

$$f_m(t) = \dot{F}_m(t)e^{-F_m(t)}, \tag{20}$$

where $F_m(t)$ is given by the auxiliary equation

$$\dot{F}_m = \theta_U I_{Uw}(t) + \theta_V I_{Vw}(t) \tag{21}$$

with initial condition $F_m(0) = 0$, while we compute $I_{Uw}(t)$ and $I_{Vw}(t)$ using (14). The use of this auxiliary equation reduces computational effort by obtaining $F_m(t)$ simultaneously with $I_{Uw}(t)$ and $I_{Vw}(t)$ (as opposed to computing the latter and then integrating).

5.3 Invasion of the variant (step 2)

Suppose that a mutant strain appears at time $t_m \geq 0$ in a single infected host, that is, with density $I_m(0) = \frac{1}{n}$, (which is effectively zero as n becomes large). Then, (2) yields $I_m(t_m) \equiv 0$ for all t, whereas the dynamics of the system follows (14). This differential equation approximation does not mean that the mutant is absent, but simply not in sufficient numbers to be visible at the coarse resolution and short time scale upon which (14) is applicable.

Then we combine (14) with a birth-and-death process approximation, $\tilde{I}_m(t)$, to the *number* of individuals infected with the mutant strain at time t after the mutant arrival time t_m, $I_m^n(t)$. We approximate the rate of new infections, $\frac{\beta_m(S_U^n(t)+\epsilon_m S_V^n(t))}{N^n(t)}$ by replacing the stochastic quantities $S_U^n(t)$, $S_V^n(t)$ and $N^n(t)$ by their deterministic approximations, giving the time-dependent birth rate

$$b_m(t) = \frac{\beta_m(S_U(t) + \epsilon_m S_V(t))}{N(t)}$$

where $S_U(t)$, $S_V(t)$ and $N(t)$ are determined via the deterministic system (14). Each death in the birth-and-death process corresponds to the removal of a susceptible, which occurs by host death or recovery at combined rate $d_m = \delta + \alpha_m + \gamma_m$. See §8.2 in the Supplementary Information of [36] for a rigorous justification.

The so-called "merciless dichotomy" [23] tells us that the time-inhomogeneous birth-and-death process started with one individual at time t_m either goes extinct, or grows without bound (i.e.

invades) with probability (see [25] and SI, Section 2)

$$P_m^{t_m} = \frac{1}{1 + \int_{t_m}^{\infty} d_m e^{-\int_{t_m}^{t} b_m(s) - d_m \, ds} \, dt}$$

Thus, either the mutant strain vanishes, or the number infected with the mutant strain will eventually be of the order of n individuals, after which we can use (1) to compute the densities of both wild-type and mutant strains.

In practice, we can compute the probability of mutant invasion when the mutant is introduced at time t_m using $P_m^{t_m} = U_m^{t_m}(\infty)$ where $U_m^{t_m}(\infty)$ is obtained via the pair of auxiliary functions $U_m^{t_m}$ and $V_m^{t_m}$ [25] defined as follows: $U_m^{t_m}(t) = \mathbb{P}\{\tilde{I}_m(t) \neq 0\}$ and $V_m^{t_m}(t) = \mathbb{P}\{\tilde{I}_m(t) = 1 \,|\, \tilde{I}_m(t) \neq 0\}$, We then have

$$\dot{U}_m^{t_m} = -d_m U_m^{t_m} V_m^{t_m} \tag{22}$$

$$\dot{V}_m^{t_m} = (d_m - b_m(t)) V_m^{t_m} - d_m (V_m^{t_m})^2, \tag{23}$$

where $U_m^{t_m}(t_m) = V_m^{t_m}(t_m) = 1$ and we compute $b_m(t)$, $S_U(t)$, $S_V(t)$ and $N(t)$, via (14). In practice, we cannot compute $U_m^{t_m}(\infty)$; to obtain an approximation we evaluate $U_m^{t_m}(t)$ for sufficiently large t that $|U_m^{t_m}(t + \Delta t) - U_m^{t_m}(t)|$ is less than our desired threshold of error.

Note that several variants can arise and fail to invade before finally a lucky variant manages to invade. We can use the probability of invasion P_m^t of a variant introduced at time t to characterize the distribution of the first time t_i at which a mutant is introduced that successfully invades. By the thinning property of Poisson point processes, we have [28]:

$$\mathbb{P}\{t_i > t\} = e^{-\int_0^t (\theta_U I_{Uw}(s) + \theta_V I_{Vw}(s)) P_m^s ds} \tag{24}$$

where $\theta_U I_{Uw}(t) + \theta_V I_{Vw}(t)$ is the flux of vaccine-escape mutants from the wild-type population. We compute numerically the probability density function g_m of the first arrival time t_i of a vaccine-

escape mutant that successfully invades using

$$g_m(t) = \dot{G}_m(t)e^{-G_m(t)}, \tag{25}$$

where $G_m(t)$ is given by the auxiliary equation

$$\dot{G}_m(t) = \left(\theta_U I_{Uw}(t) + \theta_V I_{Vw}(t)\right) P_m^t \tag{26}$$

with initial condition $G_m(0) = 0$ and computing $I_{Uw}(t)$ and $I_{Vw}(t)$ using (14).

Compare (24) with (19) and note that the probability that no vaccine-escape mutant will ever *arise* is

$$\mathbb{P}\{t_m = \infty\} = e^{-\int_0^\infty (\theta_U I_{Uw}(t) + \theta_V I_{Vw}(t))dt}.$$

In contrast, the probability that no vaccine-escape mutant will ever *invade* is the larger probability

$$\mathbb{P}\{t_i = \infty\} = e^{-\int_0^\infty (\theta_U I_{Uw}(t) + \theta_V I_{Vw}(t))P_m^t dt}.$$

Note that P_m^t converges as $t \to \infty$ to $P_m^\star = 1 - 1/R_m^\star$ which is nonzero, so that

$$\mathbb{P}\{t_m = \infty\} = 0 \Leftrightarrow \int_0^\infty (\theta_U I_{Uw}(t) + \theta_V I_{Vw}(t))dt = \infty \Leftrightarrow \mathbb{P}\{t_i = \infty\} = 0,$$

that is, the probability of adaptation is 1 if and only if $t \mapsto (\theta_U I_{Uw}(t) + \theta_V I_{Vw}(t))$ is not integrable. In other words, the probability of adaptation is 1 in the limit $t \to \infty$ when the wild type is not driven to extinction by vaccination (i.e. $\nu < \nu_c$) which implies that there is an uninterrupted flux of mutation producing vaccine-escape variants. One of these mutants will eventually escape extinction and invade. Yet, the time needed for a successful variant to appear may be very long and we focus in the main text on A_m^t the probability of adaptation before time t (equation (10) and Figure 6).

5.4 Fixation of the variant (step 3)

Suppose now that the mutant strain successfully invades; we next consider the probability P_{fix} that the mutant will outcompete the wild type and go to fixation. Fixation of the mutant occurs if it is still present when the wild-type strain disappears. If we let T_m and T_w be the extinction times of mutant and wild-type strains, the probability of mutant fixation is thus $\mathbb{P}\{T_w < T_m\}$ which we may decompose as

$$\begin{aligned}\int_{t_m}^{\infty} \mathbb{P}\{T_m > t\}\mathbb{P}\{T_w \in dt\} &= -\int_{t_m}^{\infty} \mathbb{P}\{T_m > t\}\frac{d}{dt}\mathbb{P}\{T_w > t\}\, dt \\ &= -\int_{t_m}^{\infty} \mathbb{P}\{I_m^n(t) > 0\}\frac{d}{dt}\left(1 - \mathbb{P}\{I_w^n(t) = 0\}\right)\, dt \\ &= \int_{t_m}^{\infty} \mathbb{P}\{I_m^n(t) > 0\}\frac{d}{dt}\mathbb{P}\{I_w^n(t) = 0\}\, dt.\end{aligned} \tag{27}$$

We again obtain estimates of $\mathbb{P}\{I_w^n(t) > 0\}$ and $\mathbb{P}\{I_m^n(t) > 0\}$ using the fact that conditional on $S_U(t)$, $S_V(t)$ and $N(t)$, $(\tilde{I}_w(t), \tilde{I}_m(t))$ follows a time-inhomogeneous, two-type birth-and-death process, where the birth rates for the two types, $i = w, m$, are given by

$$b_i(t) = \frac{\beta_i(S_U(t) + \epsilon_i S_V(t))}{N(t)}$$

and the death rates are $d_i = \delta + \alpha_i + \gamma_i$. The birth rates vary with time due to the epidemiological perturbations following the start of vaccination and in particular, to the feedback of mutant invasion on S_V and S_U. To quantify these epidemiological perturbations, we now approximate the density of susceptibles and total host density by the values of $S_U(t)$, $S_V(t)$ and $N(t)$ obtained from the full deterministic system (1), which accounts for the presence of the mutant by replacing I_m with its *expected value*.

We need to take care in choosing the initial conditions of (1) to account for the fact that we consider the time of appearance of the first mutant that successfully invades and so are conditioning on the non-extinction of the mutant strain, and for the inherent variability in the time required to invade; this results in a random initial condition for the deterministic dynamics (see Supplementary Information §4 for details). In practice, we find that the randomness has negligible effect, but

we must still take the conditioning into account. To do so, we first use (14) to compute the epidemiological dynamics of the wild type before the introduction of the mutant at time t_m. Then, at time t_m, we use (1) where $S_U(t_m)$, $S_V(t_m)$, $N(t_m)$ and $I_w(t_m)$ are obtained from (14) and take $I_m(t_m) = \frac{1}{(1-P_m^{t_m})n}$ (see Supplementary Information §4). Crucially, the initial density of the mutant depends on the probability of successful invasion of the mutant $P_m^{t_m}$ obtained above.

Provided we use (1) with the appropriate initial conditions as previously, the birth rates of both the wild-type and mutant strains are approximately deterministic, and from [25], we have:

$$\mathbb{P}\{I_i^n(t) > 0\} \approx \mathbb{P}\{\tilde{I}_i(t) > 0\} = 1 - (1 - U_i^{t_m}(t))^{I_i^n(t_m)}, \tag{28}$$

where

$$U_i^{t_m}(t) = \frac{1}{1 + \int_{t_m}^t d_i e^{-\int_{t_m}^u b_i(s) - d_i \, ds} \, du} \tag{29}$$

is the probability that an individual infected with strain i ($i = m, w$) present at t_m has descendants alive at time t. Under the branching assumption, the lines of descent of distinct infected individuals are independent, hence the probability that strain i vanishes by time t is the product of the probabilities that each line of descent vanishes, $(1 - U_i^{t_m}(t))^{I_i^n(t_m)}$.

In practice, we need two pairs of auxiliary equations to track the probability of extinction of both the wild type and the mutant

$$\dot{U}_w^{t_m} = -d_w U_w^{t_m} V_w^{t_m} \tag{30}$$

$$\dot{V}_w^{t_m} = (d_w - b_w(t)) V_w^{t_m} - d_w (V_w^{t_m})^2 \tag{31}$$

$$\dot{U}_m^{t_m} = -d_m U_m^{t_m} V_m^{t_m} \tag{32}$$

$$\dot{V}_m^{t_m} = (d_m - b_m(t)) V_m^{t_m} - d_m (V_m^{t_m})^2, \tag{33}$$

with $U_w^{t_m}(t_m) = V_w^{t_m}(t_m) = U_m^{t_m}(t_m) = V_m^{t_m}(t_m) = 1$. To compute the probability of fixation, we first consider the probability of fixation prior to time t, which is derived in exactly the same manner as (27).

$$U^{t_m}(t) = \int_{t_m}^t \mathbb{P}\{I_m^n(s) > 0\} \frac{d}{dt} \mathbb{P}\{I_w^n(s) = 0\} \, ds,$$

Using (28) to approximate the probabilities $\mathbb{P}\{I_m^n(s) > 0\}$ and $\mathbb{P}\{I_w^n(s) = 0\}$, we get

$$U^{t_m}(t) = \int_{t_m}^{t} [1 - (1 - U_m^{t_m}(s))^{I_m^n(t_m)}][I_w^n(t_m)(-\dot{U}_w^{t_m})(1 - U_w^{t_m}(s))^{I_w^n(t_m)-1}]ds.$$

Differentiating this and taking $I_w^n(t_m) = nI_w(t_m)$ and $I_m^n(t_m) = 1$ yields the following auxiliary equation for $U^{t_m}(t)$:

$$\dot{U}^{t_m} = nI_w(t_m)(\delta + \alpha_w + \gamma_w)U_w^{t_m}V_w^{t_m}\left(1 - U_w^{t_m}\right)^{nI_w(t_m)-1}U_m^{t_m}, \tag{34}$$

with initial condition $U^{t_m}(t_m) = 0$. We estimate the fixation probability as $P_{fix}^{t_m} = U^{t_m}(\infty)$ as above.

5.5 Invasion and Fixation with Standing Variation

We now come back to the probability of adaptation from standing variation at time $t = 0$, using the probability p_k that there are k mutants present at time $t = 0$ and the estimates for the probabilities of invasion and fixation $P_m^{t_m}$ and $P_{fix}^{t_m}$, of a single mutant arriving at time t_m, taking $t_m = 0$. Recall that p_k is negative binomial with success probability $R_m^0 = b_m^0/d_m$ and $r = \mu_m/b_m^0$ failures. Under the branching process approximation, the chain of infections started by each mutation will go extinct independently with probability $1 - P_m^0$. The probability of invasion is then the probability that at least one line survives, $1 - (1 - P_m^0)^k$. Summing this over all possible values of k gives us the invasion probability from standing variation,

$$\sum_{k=1}^{\infty} p_k\left(1 - (1 - P_m^0)^k\right) = 1 - p_0 - \sum_{k=1}^{\infty} p_k(1 - P_m^0)^k = 1 - \sum_{k=0}^{\infty} p_k(1 - P_m^0)^k.$$

Recalling that the probability generating function for the number of mutants at time $t = 0$ is

$$\sum_{k=0}^{\infty} p_k z^k = \left(\frac{1 - R_m^0}{1 - R_m^0 z}\right)^r,$$

which converges provided $|z| < \frac{1}{R_m^0}$, we see that the probability of invasion from standing variation is $1 - \left(\frac{1-R_m^0}{1-R_m^0(1-P_m^0)}\right)^r$.

Similarly, if there are k mutations at time $t = 0$, (28) gives us that $\mathbb{P}\{I_m^n(t) > 0 | I_m(0) = k\} \approx 1 - (1 - U_m^0(t))^k$, so proceeding as above, we find that the probability that the mutant is still present at time t, assuming that at least one individual was present at time $t = 0$ is approximately $1 - \left(\frac{1-R_m^0}{1-R_m^0(1-U_m^0(t))}\right)^r$. Substituting this for $\mathbb{P}\{I_m^n(t) > 0\}$ in (27) and differentiating as above gives us an auxiliary equation analogous to (34) for $U^0(t)$, the probability that the mutant fixes starting from standing variation:

$$\begin{aligned}\dot{U}^0 &= \mathbb{P}\{I_m^n(s) > 0\}\frac{d}{dt}\mathbb{P}\{I_w^n(s) = 0\} \\ &= nI_w(0)(\delta + \alpha_w + \gamma_w)U_w^0 V_w^0 \left(1 - U_w^0\right)^{nI_w(0)-1}\left(1 - \left(\frac{1 - R_m^0}{1 - R_m^0(1 - U_m^0)}\right)^r\right).\end{aligned}$$

As previously, we obtain $P_{fix}^0 = \dot{U}^0(\infty)$ by choosing t sufficiently large that $\dot{U}^0(t)$ equilibrates.

5.6 Stochastic simulations

We carried out stochastic simulations to check the validity of our results. We developed an individual-based simulation program for the Markov process described in **Table S1**. In order to match the assumption used in our analysis we start the simulation when the system is at its endemic equilibrium before vaccination given by equation (11) in section 5.1. Then we introduce a single host infected with the mutant pathogen at a time t_m after the start of vaccination and we let the simulation run until one of the pathogen variants (the wild-type or the mutant) goes extinct. If the wild-type goes extinct first we record this run as a "mutant fixation event". We ran 1000 replicates for each set of parameters and we plot the proportion of runs that led to mutant fixation in **Figure 5**. We also used our simulations to confirm our prediction on the speed of viral adaptation (**Figure 6**). In this scenario we allowed the vaccine-escape variant to be introduced by mutation from the wild-type genotype as detailed in section 5.1. We carried out 1000 simulations and monitored (i) the frequency of the escape mutant at different points in time after the start of vaccination (**Figure 6A**) (ii) the number of introduction events by mutation and (**Figure 6B**).

We also used this simulation approach to go beyond the scenarios used in our analysis to check

the robustness of some of our results. We developed a modified version of our simulation approach to relax two simplifying assumptions used throughout our analysis: (i) vaccination starts when the epidemiology has reached an endemic equilibrium, (ii) naturally immune host are fully protected against reinfection.

• **The timing of the start of vaccination:** We used a modified version of our simulation code to explore the robustness of our results when vaccination starts sooner and the wild-type pathogen has not reached its endemic equilibrium. In practice, we start the simulation with n hosts where a fraction $f = 0.1\%, 1\%$ or 10% is infected by the wild-type (i.e. $I_w^n(0) = fn$ and $S^n(0) = (1-f)n$). Vaccination rollout is assumed to start at time $t = 0$. We introduce an infected host with a mutant pathogen at time t_m and we monitor its dynamics to obtain the probability of invasion from 1000 independent replicates. Starting vaccination when the incidence is low tends to increase the probability of invasion of the escape mutant because it is less likely to go extinct when the density of susceptible hosts is more abundant (**Figure S5**). Note, however, that this effect is maximised when the mutant is introduced soon after the start of vaccination (i.e. low values of t_m). Indeed, for the parameter values we used, the endemic equilibrium is reached very fast and the predictions of the probability of invasion computed when vaccination starts at the endemic equilibrium remain relatively good.

• **Efficacy of natural immunity against reinfections:** We used a modifier version of our simulation code to explore the robustness of our results when naturally immune hosts are not perfectly protected. In this scenario we assume that recovered hosts can be reinfected by strain i at a rate $\rho\epsilon_i \frac{I_i}{N}$. In this scenario, it is still possible to aggregate the density of different types of hosts infected by the same strain i, $I_i := I_{Ui} + I_{Ui} + I_{Ri}$, which modifies the effective per-generation reproduction ratio:

$$R_i^e = R_i \left(\frac{S_U}{N} + \epsilon_i \frac{S_V}{N} + \rho\epsilon_i \frac{R}{N} \right)$$

Hence, higher values of ρ give an extra advantage to the escape mutant because it increases the fraction of imperfectly immune hosts. This new expression of the effective per-generation reproduction ratio can be used to derive a good approximation of the probability of mutant invasion using (9). This approximation fully captures how higher values of ρ increase the probability of invasion

of escape mutations (**Figure S6**). Interestingly, when ρ is large, the probability of invasion is less sensitive to the time at which the escape mutant is introduced because, whatever the time after the start of vaccination, the fraction of imperfectly immune host is large.

The simulation code is available upon request and will be deposited on zenodo after acceptance of the manuscript.

Acknowledgements: SG acknowledges support from the CNRS PEPS 2022 grant "VaxDurable".

References

[1] Helen K Alexander and Sebastian Bonhoeffer. Pre-existence and emergence of drug resistance in a generalized model of intra-host viral dynamics. *Epidemics*, 4(4):187–202, 2012.

[2] Helen K Alexander, Guillaume Martin, Oliver Y Martin, and Sebastian Bonhoeffer. Evolutionary rescue: linking theory for conservation and medicine. *Evolutionary applications*, 7(10):1161–1179, 2014.

[3] H. Andersson and T. Britton. *Stochastic Epidemic Models and their Statistical Analysis*, volume 151 of *Lecture notes in statistics*. Springer, New York, 2000.

[4] Graham Bell. Evolutionary rescue. *Annual Review of Ecology, Evolution, and Systematics*, 48:605–627, 2017.

[5] Yuhua Cai and Stefan A. H. Geritz. Resident-invader dynamics of similar strategies in fluctuating environments. 2020.

[6] Philippe Carmona and Sylvain Gandon. Winter is coming: Pathogen emergence in seasonal environments. *PLoS computational biology*, 16(7):e1007954, 2020.

[7] Hélène Chabas, Sébastien Lion, Antoine Nicot, Sean Meaden, Stineke van Houte, Sylvain Moineau, Lindi M Wahl, Edze R Westra, and Sylvain Gandon. Evolutionary emergence of infectious diseases in heterogeneous host populations. *PLoS biology*, 16(9):e2006738, 2018.

[8] Sarah Cobey, Daniel B Larremore, Yonatan H Grad, and Marc Lipsitch. Concerns about sars-cov-2 evolution should not hold back efforts to expand vaccination. *Nature Reviews Immunology*, pages 1–6, 2021.

[9] Nicholas G Davies, Sam Abbott, Rosanna C Barnard, Christopher I Jarvis, Adam J Kucharski, James D Munday, Carl AB Pearson, Timothy W Russell, Damien C Tully, Alex D Washburne, et al. Estimated transmissibility and impact of sars-cov-2 lineage b. 1.1. 7 in england. *Science*, 372(6538), 2021.

[10] Troy Day, David A Kennedy, Andrew F Read, and Sylvain Gandon. Pathogen evolution during vaccination campaigns. *PLoS Biology*, 20(9):e3001804, 2022.

[11] Troy Day and Andrew F Read. Does high-dose antimicrobial chemotherapy prevent the evolution of resistance? *PLoS computational biology*, 12(1):e1004689, 2016.

[12] Saad-Roy et al. Epidemiological and evolutionary considerations of sars-cov-2 vaccine dosing regimes. *medRxiv*, 2020.

[13] S. Gandon and T. Day. The evolutionary epidemiology of vaccination. *J. Royal Soc. Interface*, 4(16):803–817, 2007.

[14] Sylvain Gandon and Troy Day. Evidences of parasite evolution after vaccination. *Vaccine*, 26:C4–C7, 2008.

[15] Sylvain Gandon and Sébastien Lion. Targeted vaccination and the speed of sars-cov-2 adaptation. *medRxiv*, 2021.

[16] Sylvain Gandon, Margaret Mackinnon, Sean Nee, and Andrew Read. Imperfect vaccination: some epidemiological and evolutionary consequences. *Proceedings of the Royal Society of London. Series B: Biological Sciences*, 270(1520):1129–1136, 2003.

[17] S. A. H. Geritz. Resident-invader dynamics and the coexistence of similar strategies. *J. Math. Biol.*, 50(1):67–82, 2005.

[18] Philip J Gerrish, Fernando Saldana, Benjamin Galeota-Sprung, Alexandre Colato, Erika E Rodriguez, and Jorge X Velasco-Hernandez. How unequal vaccine distribution promotes the evolution of vaccine escape. *Available at SSRN 3827009*, 2021.

[19] Bryan Grenfell, Nicole Mideo, Laura C Pollitt, Andrew F Read, David L Smith, Claire Standley, Nina Wale, Geoffrey Chi-Johnston, Ted Cohen, Troy Day, et al. The path of least resistance: aggressive or moderate. 2014.

[20] Bryan T Grenfell, Oliver G Pybus, Julia R Gog, James LN Wood, Janet M Daly, Jenny A Mumford, and Edward C Holmes. Unifying the epidemiological and evolutionary dynamics of pathogens. *science*, 303(5656):327–332, 2004.

[21] Matthew Hartfield and Samuel Alizon. Within-host stochastic emergence dynamics of immune-escape mutants. *PLoS computational biology*, 11(3):e1004149, 2015.

[22] Jan Humplik, Alison L Hill, and Martin A Nowak. Evolutionary dynamics of infectious diseases in finite populations. *Journal of theoretical biology*, 360:149–162, 2014.

[23] P. Jagers. Stabilities and instabilities in population dynamics. *J. Appl. Prob.*, pages 770–780, 1992.

[24] S. Karlin and J. McGregor. Linear growth, birth and death processes. *J. Math. & Mech.*, 7(4):643–662, 1958.

[25] D. G. Kendall. On the generalized "Birth-and-Death" process. *Ann. Math. Stat.*, 19(1):1–15, 1948.

[26] David A Kennedy and Andrew F Read. Why does drug resistance readily evolve but vaccine resistance does not? *Proceedings of the Royal Society B: Biological Sciences*, 284(1851):20162562, 2017.

[27] David A Kennedy and Andrew F Read. Why the evolution of vaccine resistance is less of a concern than the evolution of drug resistance. *Proceedings of the National Academy of Sciences*, 115(51):12878–12886, 2018.

[28] John Frank Charles Kingman. *Poisson processes*, volume 3. Clarendon Press, 1992.

[29] Oleg Kogan, Michael Khasin, Baruch Meerson, David Schneider, and Christopher R Myers. Two-strain competition in quasineutral stochastic disease dynamics. *Physical Review E*, 90(4):042149, 2014.

[30] T. G. Kurtz. *Approximation of Population Processes*, volume 36. Society for Industrial and Applied Mathematics, Philadelphia, 1981.

[31] Gabriela Lobinska, Ady Pauzner, Arne Traulsen, Yitzhak Pilpel, and Martin A Nowak. Evolution of resistance to covid-19 vaccination with dynamic social distancing. *Nature human behaviour*, 6(2):193–206, 2022.

[32] Guillaume Martin, Robin Aguilée, Johan Ramsayer, Oliver Kaltz, and Ophélie Ronce. The probability of evolutionary rescue: towards a quantitative comparison between theory and evolution experiments. *Philosophical Transactions of the Royal Society B: Biological Sciences*, 368(1610):20120088, 2013.

[33] Hamish McCallum, Nigel Barlow, and Jim Hone. How should pathogen transmission be modelled? *Trends in ecology & evolution*, 16(6):295–300, 2001.

[34] AngelaR McLean. After the honeymoon in measles control. *The Lancet*, 345(8945):272, 1995.

[35] David V McLeod, Lindi M Wahl, and Nicole Mideo. Mosaic vaccination: how distributing different vaccines across a population could improve epidemic control. *bioRxiv*, pages 2020–11, 2021.

[36] T. L. Parsons, A. Lambert, T. Day, and S. Gandon. Pathogen evolution in finite populations: slow and steady spreads the best. *J. Royal Soc. Interface*, 15(147), 2018.

[37] Robert S Paton, Christopher E Overton, and Thomas Ward. The rapid replacement of the delta variant by omicron (b. 1.1. 529) in england. *Sci. Transl. Med.*, page eabo5395, 2022.

[38] Tadeas Priklopil and Laurent Lehmann. Invasion implies substitution in ecological communities with class-structured populations. 134:36–52, 2020.

[39] Jason W Rausch, Adam A Capoferri, Mary Grace Katusiime, Sean C Patro, and Mary F Kearney. Low genetic diversity may be an achilles heel of sars-cov-2. *Proceedings of the National Academy of Sciences*, 117(40):24614–24616, 2020.

[40] Andrew F Read, Troy Day, and Silvie Huijben. The evolution of drug resistance and the curious orthodoxy of aggressive chemotherapy. *Proceedings of the National Academy of Sciences*, 108(Supplement 2):10871–10877, 2011.

[41] Simon A Rella, Yuliya A Kulikova, Emmanouil T Dermitzakis, and Fyodor A Kondrashov. Rates of sars-cov-2 transmission and vaccination impact the fate of vaccine-resistant strains. *Scientific Reports*, 11(1):1–10, 2021.

[42] Olivier Restif and Bryan T Grenfell. Vaccination and the dynamics of immune evasion. *Journal of the Royal Society Interface*, 4(12):143–153, 2007.

[43] Rafael Sanjuán, Miguel R Nebot, Nicola Chirico, Louis M Mansky, and Robert Belshaw. Viral mutation rates. *Journal of virology*, 84(19):9733–9748, 2010.

[44] Robin N Thompson, Edward M Hill, and Julia R Gog. Sars-cov-2 incidence and vaccine escape. *The Lancet Infectious Diseases*, 2021.

[45] Stineke van Houte, Alice KE Ekroth, Jenny M Broniewski, Hélène Chabas, Ben Ashby, Joseph Bondy-Denomy, Sylvain Gandon, Mike Boots, Steve Paterson, Angus Buckling, et al. The diversity-generating benefits of a prokaryotic adaptive immune system. *Nature*, 532(7599):385–388, 2016.

[46] Erik Volz, Swapnil Mishra, Meera Chand, Jeffrey C Barrett, Robert Johnson, Lily Geidelberg, Wes R Hinsley, Daniel J Laydon, Gavin Dabrera, Áine O'Toole, et al. Assessing transmissibility of sars-cov-2 lineage b. 1.1. 7 in england. *Nature*, 593(7858):266–269, 2021.

[47] Pengfei Wang, Manoj S Nair, Lihong Liu, Sho Iketani, Yang Luo, Yicheng Guo, Maple Wang, Jian Yu, Baoshan Zhang, Peter D Kwong, et al. Antibody resistance of sars-cov-2 variants b. 1.351 and b. 1.1. 7. *Nature*, pages 1–6, 2021.

Table 1: Parameters and dynamical variables of the model

Symbol	Description	Default value
Parameters		
λ	influx rate of susceptible hosts	$3\ 10^{-4}\ week^{-1}$
δ	natural death rate of hosts	$3\ 10^{-4}\ week^{-1}$
ω_R	rate of waning immunity of naturally immune hosts	$0.05\ week^{-1}$
ω_V	rate of waning immunity of vaccinated hosts	$0.05\ week^{-1}$
p	probability of vaccination of newborns	0
ν	rate of vaccination rollout	variable
θ_U	rate of mutation (from w to m) in unvaccinated hosts	variable
θ_V	rate viral mutation (from w to m) in vaccinated hosts	variable
n	system size (scaling parameter allowing us to manipulate the pathogen population size)	variable
α_w	virulence (increased mortality rate) by strain w	$0.02\ week^{-1}$
β_w	rate of transmission of viral strain w	$10\ week^{-1}$
γ_w	recovery rate of the host infected by strain w	$2\ week^{-1}$
ϵ_w	probability of infection of vaccinated hosts by strain w	0.05
α_m	virulence (increased mortality rate) by strain m	*variable*
β_m	rate of transmission of viral strain w	*variable*
γ_m	recovery rate of the host infected by strain m	$2\ week^{-1}$
ϵ_m	probability of infection of vaccinated hosts by strain m	1
Variables		
S_U	density of unvaccinated susceptible hosts	
S_V	density of vaccinated susceptible hosts	
R	density of naturally immune hosts	
I_{Ui}	density of unvaccinated hosts infected by strain $i \in (w, m)$	
I_{Vi}	density of vaccinated hosts infected by strain $i \in (w, m)$	

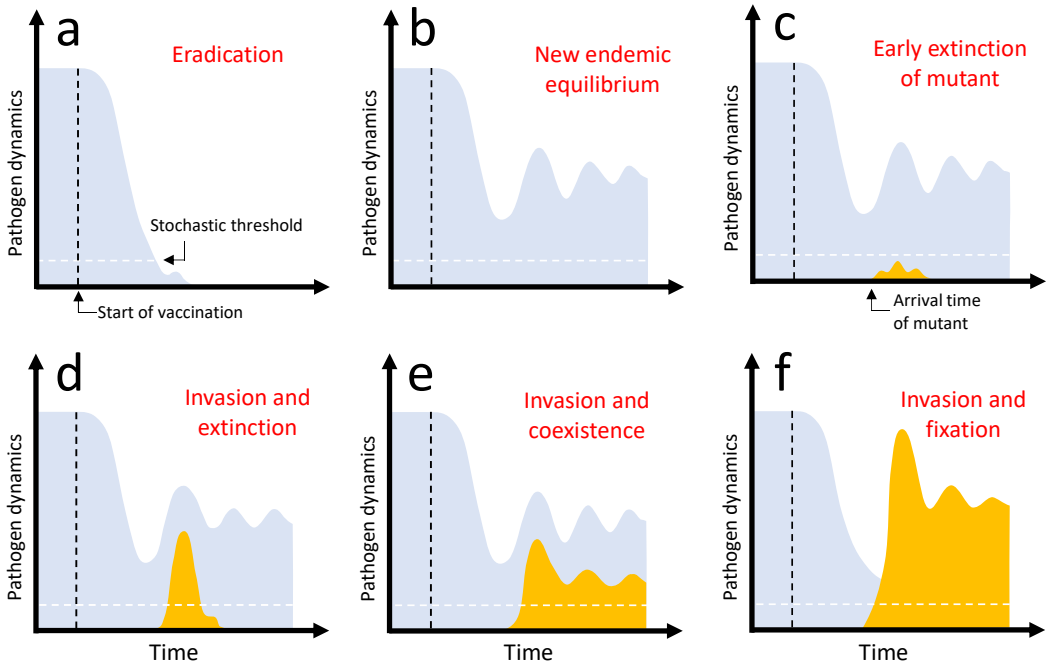

Figure 1: Graphical representation of the different evolutionary epidemiology outcomes after vaccination. The density of the wild-type pathogen is indicated in light blue and the dynamics of the mutant in orange. Each panel describes the temporal dynamics of the epidemics after the start of vaccination: (a) eradication of the wild-type pathogen, (b) new endemic equilibrium of the wild-type population after damped oscillations (with no introduction of the vaccine-escape mutant), (c) early extinction of the vaccine-escape mutant after its introduction by mutation, (d) invasion of the vaccine-escape mutant followed by the its extinction, (e) invasion of the vaccine-escape mutant and long-term coexistence with the wild type in a new endemic equilibrium after damped oscillations, (f) invasion and fixation of the vaccine-escape mutant (extinction of the wild type). The vertical dashed line (black) indicates the start of vaccination. For simplicity we consider that vaccination starts after the wild-type population has reached an endemic equilibrium. The horizontal dashed line indicates the "stochastic threshold" above which one may consider that the deterministic model provides a very good approximation of the dynamics and we can neglect the effect of demographic stochasticity. *Invasion* occurs when the vaccine-escape variant manages to go beyond the "stochastic threshold" (panels d, e and f). *Adaptation* occurs when the vaccine-escape variant is maintained in the population (panels e and f). *Fixation* occurs when the vaccine-escape variant manages to outcompete the wild type (panel f).

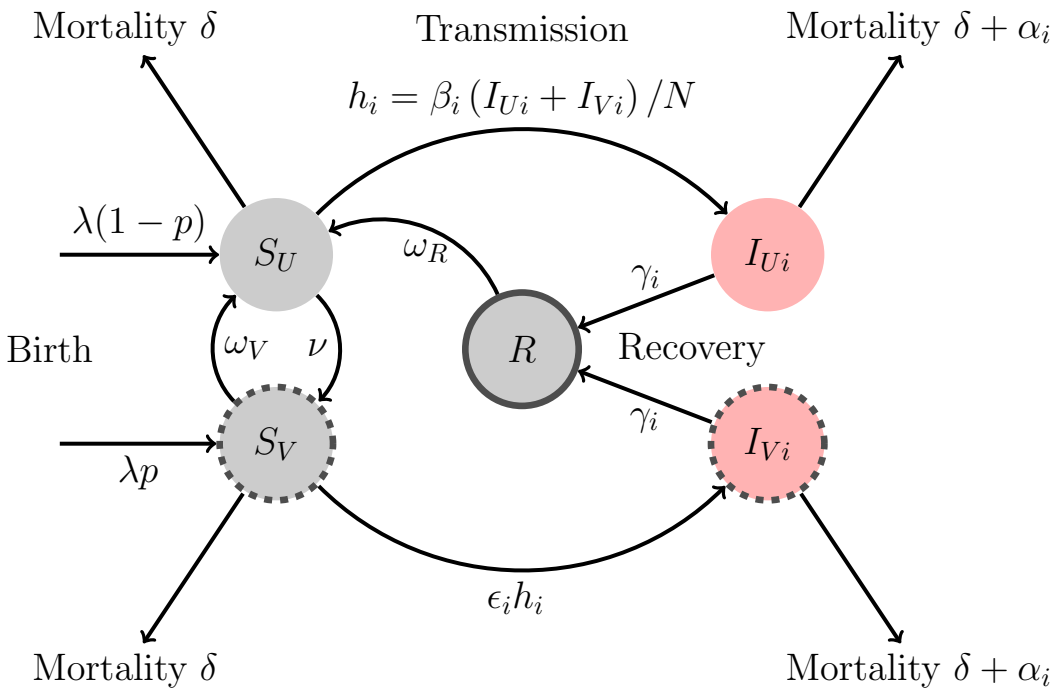

Figure 2: A schematic representation of the model. Naive and uninfected hosts (S_U hosts) are introduced at a rate λ and are vaccinated with probability p at birth and at rate ν later on. Immunization induced by the vaccine wanes at rate ω_V. Uninfected hosts (S_U and S_V) die at a rate δ while infected hosts (I_{Ui} and I_{Vi}) die at a rate $d_i = \delta + \alpha_i$, where i refers to the virus genotype: the wild-type ($i = w$) or the vaccine-escape mutant ($i = m$). The rate of infection of naive hosts by the genotype i is $h_i = \beta_i(I_{Ui} + I_{Vi})/N$, where β_i is the transmission rate of the genotype i. Vaccination reduces the force of infection and ϵ_i refers to the ability of the genotype i to escape the immunity triggered by vaccination (we assume $\epsilon_m > \epsilon_w$). A host infected by parasite genotype i recovers from the infection at rate γ_i and yields naturally immune hosts (R hosts) that cannot be reinfected by both the wild-type and the escape mutant. Natural immunity is assumed to wane at rate ω_R. The total host population density is $N = S_U + S_V + \sum_i (I_{Ui} + I_{Vi}) + R$.

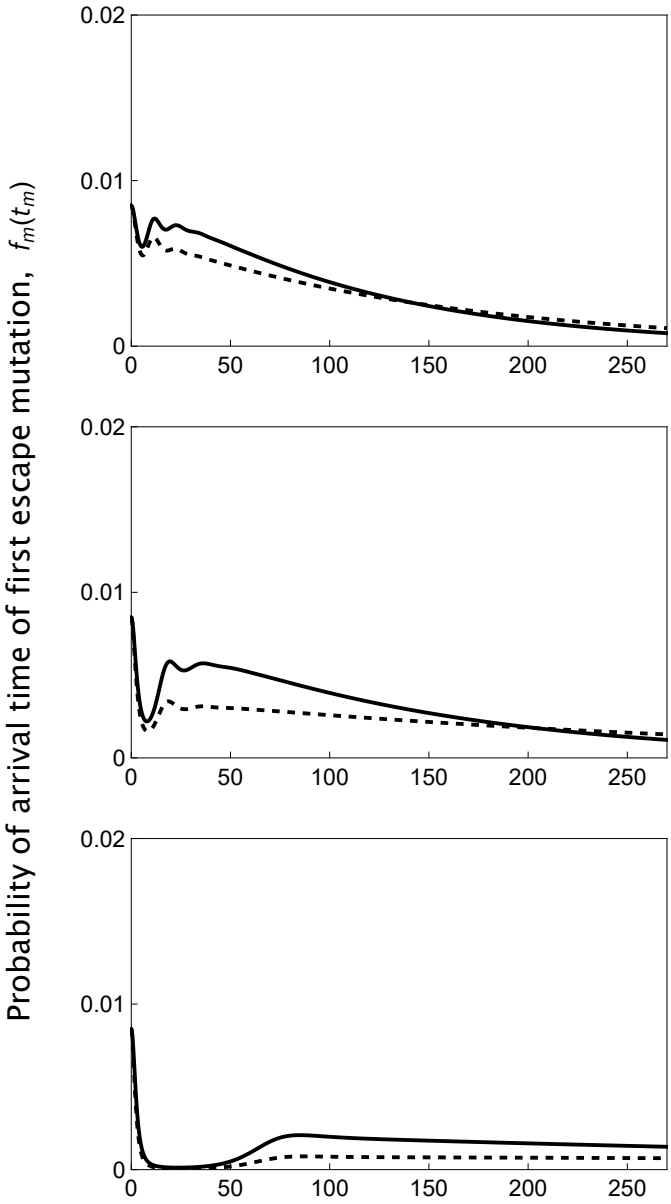

Figure 3: Faster vaccine rollout delays the arrival time of the first escape mutant. We plot the probability density function $f_m(t)$ of the arrival time of the first escaoe mutant for different speeds of vaccination rollout: $\nu = 0.05$ (top), 0.15 (middle) and 0.24 (bottom). We contrast a scenario where $\theta_V = \theta_U$ (dashed line), and $\theta_V = 10 \times \theta_U$ (full line). Other parameter values: $\theta_U = 1$, $\lambda = \delta = 3\ 10^{-4}$, $\omega_V = \omega_R = 0.05$, $p = 0$, $\alpha_w = 0.02$, $\beta_w = 10$, $\gamma_w = 2$, $\epsilon_w = 0.05$, $R_w = 4.95$. For these parameter values the critical rate of vaccination ν_c above which the wild-type pathogen is driven to extinction is $\nu_c \approx 0.264$ (see equation (5)).

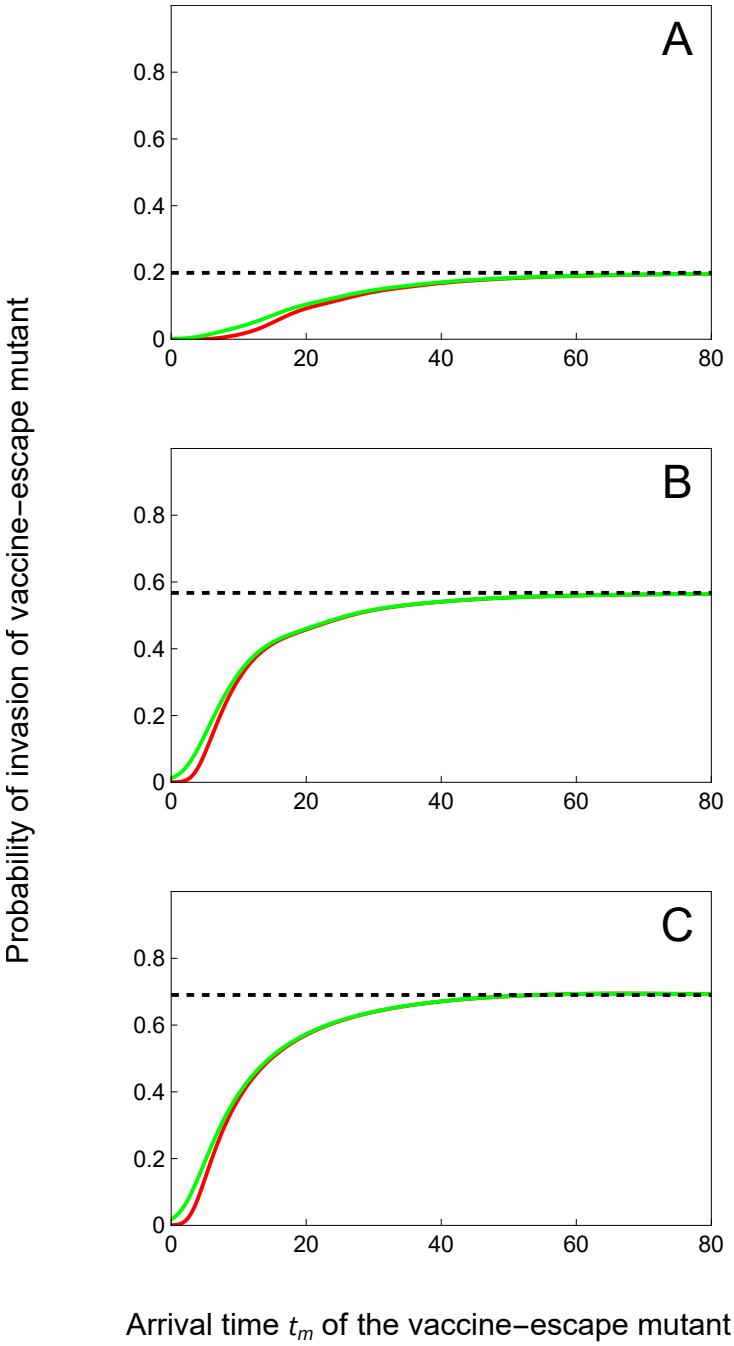

Figure 4: Probability of invasion of the vaccine-escape mutant increases with t_m. We plot the probability invasion $P_m^{t_m}$ of a *slow* (green) and a *fast* (red) vaccine-escape mutant for different speeds of vaccination rollout: $\nu = 0.05$ (top), 0.15 (middle) and 0.24 (bottom). The *slow* mutant: $\alpha_m = 0.02, \beta_m = 7, \gamma_m = 2, \epsilon_m = 1, R_m = 3.46$. The *fast* mutant: $\alpha_m = 4.0606, \beta_m = 21, \gamma_m = 2, \epsilon_m = 1, R_m = 3.46$. The probability of invasion $P_m^\star$ in the limit $t_m \to \infty$ (see equation (9)) is indicated with the dashed black line. Other parameter values as in **Figure 3**: $\lambda = \delta = 3\ 10^{-4}$, $\omega_V = \omega_R = 0.05$, $p = 0$, $\alpha_w = 0.02$, $\beta_w = 10$, $\gamma_w = 2$, $\epsilon_w = 0.05$, $R_w = 4.95$.

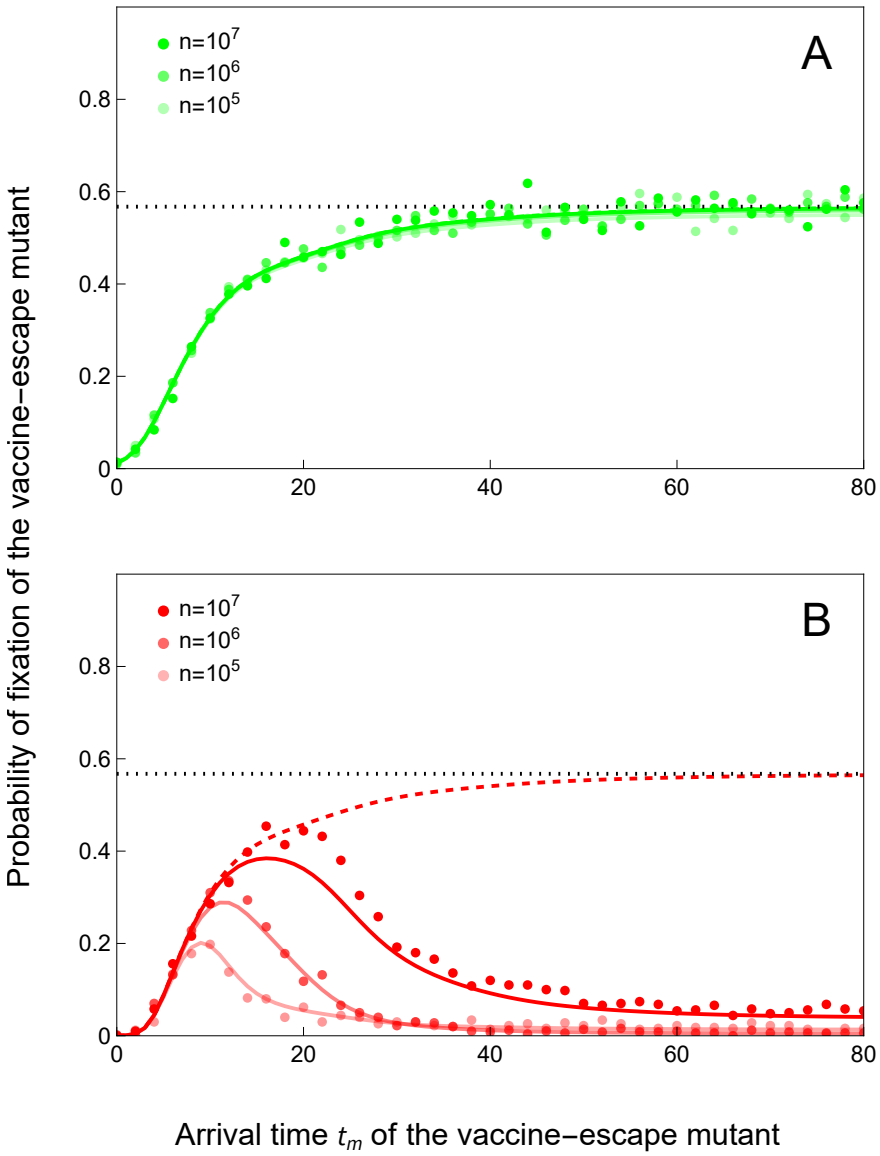

Figure 5: Probability of fixation of the vaccine-escape mutant may be low when t_m is large. We plot the probability of fixation of (A) a *slow* (green) and (B) a *fast* (red) vaccine-escape mutant for an intermediate speed of vaccination rollout: $\nu = 0.15$. The *slow* mutant: $\alpha_m = 0.02, \beta_m = 7, \gamma_m = 2, \epsilon_m = 1, R_m = 3.46$. The *fast* mutant: $\alpha_m = 4.0606, \beta_m = 21, \gamma_m = 2, \epsilon_m = 1, R_m = 3.46$. The full colored lines give the probability of fixation $P_{fix}^{t_m}$ computed numerically (see Methods section 5.4) and the dots give the results of individual-based simulations (see Methods section 5.6) for different values of n which affect the pathogen population size and the intensity of demographic stochasticity. We plot the probability of *invasion* $P_m^{t_m}$ (see **Figure 4**) with dashed colored line and its asymptotic value $P_m^\star$ with a dotted black line. Other parameter values as in **Figure 3**: $\lambda = \delta = 3\ 10^{-4}$, $\omega_V = \omega_R = 0.05$, $p = 0$, $\alpha_w = 0.02$, $\beta_w = 10$, $\gamma_w = 2$, $\epsilon_w = 0.05$, $R_w = 4.95$.

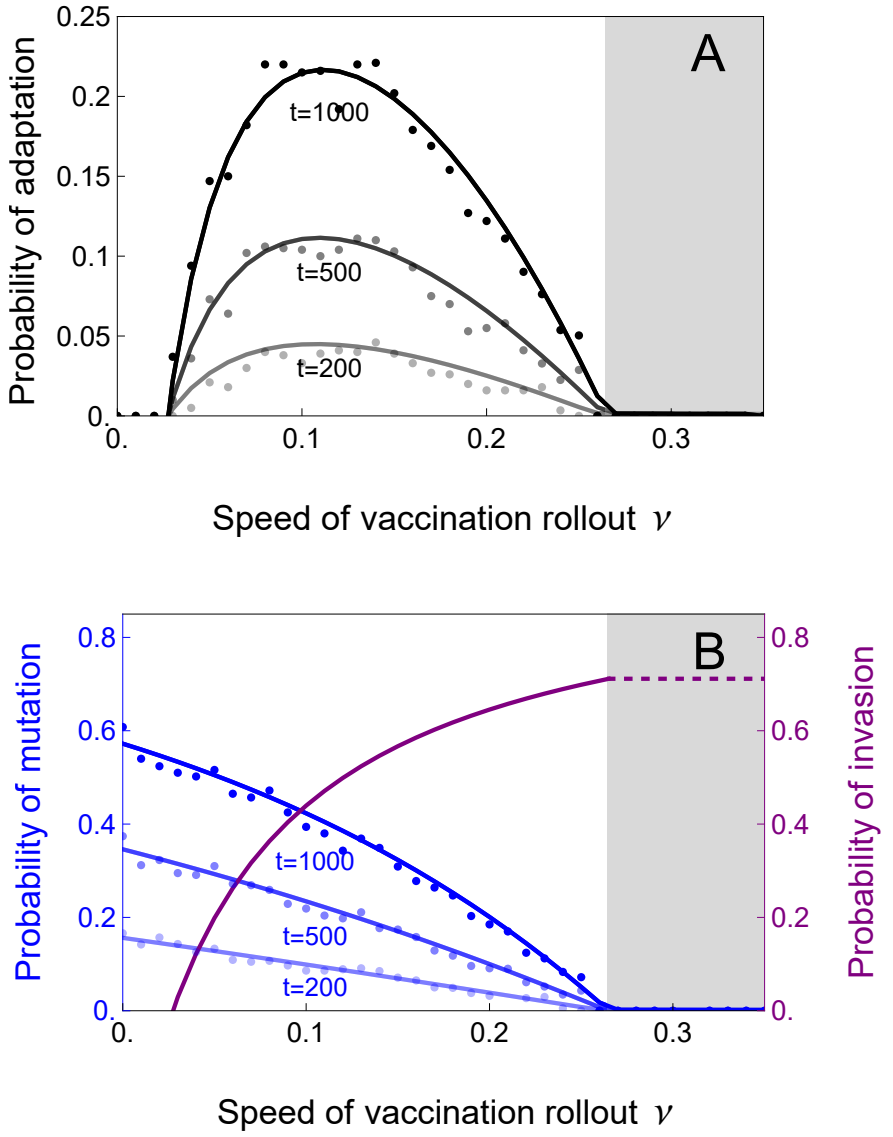

Figure 6: The probability of adaptation is maximised for intermediate speed of vaccination rollout. In (A) We plot the probability of adaptation A_m^t (black lines) against the speed of vaccination rollout at different points in time. In (B) we plot the probability M_m^t of the introduction of at least one mutant before different points in time t (blue lines) and the probability $P_m^\star$ (purple line) which gives a good approximation of the probability of successful invasion of an escape-mutant. The dashed purple line gives the probability of invasion of the escape-mutant in the absence of the wild type. The dots give the results of individual-based simulations (see Methods section 5.6). The vaccine-escape mutant is assumed to have the following phenotype (*slow* mutant in **Figure 4** and **5**): $\alpha_m = 0.02, \beta_m = 7, \gamma_m = 2, \epsilon_m = 1, R_m = 3.46$. Other parameter values: $\lambda = \delta = 3\ 10^{-4}$, $n = 10^6$, $\omega_V = \omega_R = 0.05$, $p = 0$, $\alpha_w = 0.02$, $\beta_w = 10$, $\gamma_w = 2$, $\epsilon_w = 0.05$, $R_w = 4.95$. The light gray area on the right-hand-side indicates the speed above which the wild-type pathogen is expected to be driven to extinction ($\nu > \nu_c \approx 0.264$, see equation (5)).